THE ASTROPHYSICAL JOURNAL, 473:L119–L121, 1996 December 20


# DETECTION OF AN IRRADIATED PULSAR COMPANION

B. W. STAPPERS AND M. S. BESSELL
Mount Stromlo and Siding Spring Observatories, Institute of Advanced Studies, Australian National University, Private Bag, Weston Creek, ACT 2611, Australia

AND

M. BAILES
Physics Department, University of Melbourne, Parkville, Vic 3052, Australia; and Australia Telescope National Facility, CSIRO, P.O. Box 76, Epping, NSW 2121, Australia

*Received 1996 June 12; accepted 1996 October 9*

## ABSTRACT

We have detected the optical companion of the eclipsing millisecond pulsar J2051−0827. The amplitude of the companion's light curve is at least 1.2 mag, and the variation is consistent with the companion's rotating synchronously about the pulsar and one side being heated by the impinging pulsar flux. PSR J2051−0827 is only the second pulsar binary for which direct heating of the companion has been observed. The $R$ magnitude at maximum brightness is 22.3, but we failed to detect any flux from the companion at the phase corresponding to radio eclipse. The absolute magnitude and color temperature suggest that the companion fills its Roche lobe.

*Subject headings:* binaries: eclipsing — pulsars: individual (PSR J2051−0827) — stars: neutron

## 1. INTRODUCTION

One of the most crucial issues concerning eclipsing radio pulsars is whether they will soon become isolated millisecond pulsars or will remain with their low-mass orbital companions for billions of years (Rasio, Shapiro, & Teukolsky 1989; van den Heuvel & van Paradijs 1988; Bhattacharya & van den Heuvel 1991). The answer to this puzzle lies in the mass-loss rate of the companion and the timescale for orbital evolution. At the time of the discovery of PSR B1957+20 (Fruchter, Stinebring, & Taylor 1988), it was thought that it provided the "missing link" between solitary millisecond pulsars and low-mass X-ray binaries, and that the eclipse of the pulsar resulted from matter being ablated from the companion by the pulsar's emission. It was assumed that we had been lucky to find a pulsar annihilating its companion, and that it would, on a timescale short compared to its lifetime as a radio pulsar, become a solitary millisecond pulsar. However, subsequent observations of the 20 cm continuum radiation (Fruchter & Goss 1992) and the dispersive delays near the eclipse boundaries (Ryba & Taylor 1991) indicated that the companion may not be being ablated at a rate sufficient to produce a solitary millisecond pulsar.

It is possible that the companion may be filling its Roche lobe, thus greatly increasing the mass-loss rate (Fruchter & Goss 1992; Banit & Shaham 1992). The variable orbital period derivative of PSR B1957+20 (Ryba & Taylor 1991; Arzoumanian, Fruchter, & Taylor 1994) may also be most easily explained by a Roche lobe–filling companion undergoing tidal forces caused by mass loss (Applegate & Shaham 1994). Original estimates of the companion's radius indicated that it was much smaller than its Roche limit (Fruchter et al. 1988a; Djorgovski & Evans 1988), but a revision of the dispersion-measure distance relation (Taylor & Cordes 1993) increased the distance to the system and the radius is now consistent with its filling its Roche lobe. The best-fitting model of the orbital light curve based on the impinging pulsar flux, companion radius, inclination, and intrinsic companion luminosity of Callanan, van Paradijs, & Rengelink (1995) also has the companion almost filling its Roche lobe.

The discovery of a second eclipsing binary millisecond pulsar system in the Galactic disk (Stappers et al. 1996) provided an excellent opportunity to try to detect the eclipsing star optically. PSR J2051−0827 is a 4.5 ms pulsar in a circular 2.4 hr binary orbit. The very low mass companion (minimum mass $m_c \approx 0.027\ M_\odot$) is only 1 $R_\odot$ from the pulsar. The compact nature of the system and the high Galactic latitude suggested that the companion should be detectable despite the pulsar's having a lower spin-down energy than PSR B1957+20. This Letter describes the discovery of the pulsar companion at optical wavelengths and the implications for the binary system.

## 2. OBSERVATIONS AND ASTROMETRY

A faint source was detected at the nominal position of the pulsar in observations made at the 3.9 m Anglo-Australian Telescope (AAT) of the Anglo-Australian Observatory (AAO) on 1995 July 26. Images were obtained at the prime focus using the central 500 × 500 region of a Tek 1024 charge-coupled device (CCD) giving a field of view of 3.3 arcmin$^2$ with a pixel scale of 0″.38. The CCD was used in fast read-out mode to limit the down time between observations, and the total read-out noise was minimal compared to the sky noise. The whole 2.4 hr orbital period of the binary pulsar was sampled in the $R$ band, but only partial phase coverage was possible in the $I$ band because of intermittent cloud. The seeing was typically 1″.5.

An accurate knowledge of the orbital phase of the pulsar meant that we were able to predict how the companion's brightness should vary, were it in synchronous rotation about the pulsar with one side heated by the impinging pulsar flux. During the $R$-band observations, an object near the pulsar position was seen to vary in this way, as shown in Figure 1.

To confirm the position of this variable object, the equatorial positions of 13 stars that were on the AAT frame were extracted from the COSMOS/UKST Southern Sky Catalogue of the AAO. The corresponding $x$-$y$ centers for these stars and

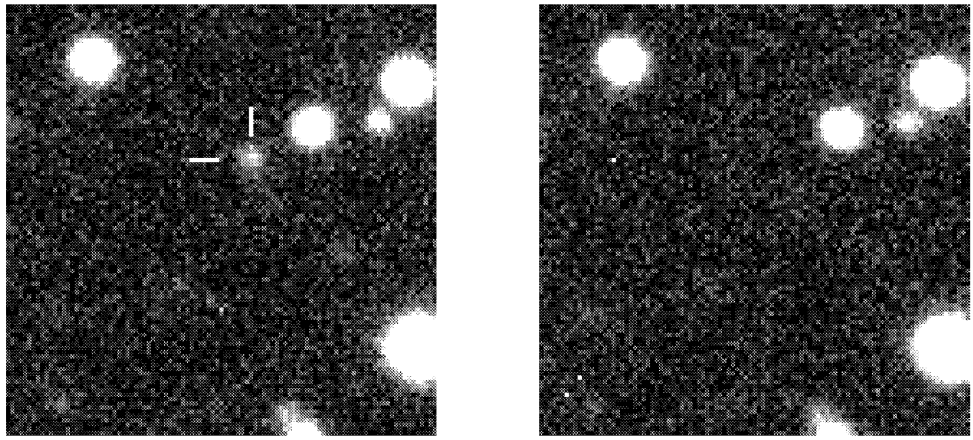

FIG. 1.—Field of PSR J2051−0827 observed in the *R* band at orbital phases 0.76 and 0.27. The companion star was not detected in the 15 minute integration time near the radio eclipse at phase 0.25.

the candidate star were measured on the frame by fitting their point-spread functions. An astrometric solution was obtained for these positions using the Starlink ASTROM package. The radial rms uncertainty in the positions was 0.″35. The measured position of the candidate is $20^h51^m07^s.515$, $-08°27'37''.25$ (J2000), which is 0.″56 away from the radio position $20^h51^m07^s.118$, $-08°27'37''.77$ (J2000) (Stappers et al. 1996). To the limiting magnitudes of $R < 23.5$ and $I < 23.3$, the next nearest star (Fig. 1) is 6.″5 from the pulsar position. The near-coincidence of the radio and optical positions and the variability of the candidate star make the identification with PSR J2051−0827 certain.

## 3. THE COMPANION'S LIGHT CURVE

To measure the *RI* magnitudes of the companion and standard stars, the IRAF implementation of DAOPHOT was used. All frames were debiased and flat-fielded using IRAF. The *I* frames contained a significant degree of fringing, and night-sky flats were made from the offset object frames to remove this effect. The standard field Mark A (Landolt 1992; Bessell 1995a) was observed at the beginning of the night to define the magnitude zero point, and local nonvarying standards on the object frames were used to define the frame-to-frame baseline. The resultant transformations were accurate to 0.01 mag. Aperture corrections were calculated using bright stars with well-defined point-spread functions in the field of the companion.

As PSR J2051−0827 lies well away from the Galactic plane ($b \sim -30°$), the extinction is expected to be low. The color excess derived from H I and galaxy counts in the region of the pulsar is $E(B-V) \approx 0.03$–$0.06$ mag (Burstein & Heiles 1982). Using the transformations of Savage & Mathis (1979), this suggests that the absorption in the two bands is $A_R \approx 0.090$ and $A_I \approx 0.045$. Thus we need not apply an extinction correction, as these small values for the absorption coefficients correspond to the maximum extinction in the direction of the source and the system is very nearby.

The brightest and faintest detected *R* magnitudes are $22.3 \pm 0.06$ and $23.2 \pm 0.1$, respectively. Apparent magnitudes of all detections in both filters are shown in Table 1. A number of frames were taken in *R* where the companion was not detected down to the limiting magnitude of ∼23.5, and these upper limits are represented by the arrows in Figure 2. The *R* light curve is symmetrical about pulsar antieclipse. An integration time of 15 minutes, which was required to try to sample the light curve with reasonable resolution and still enable detection of the companion, is still long compared to the timescale for the variability of the companion magnitude. Hence, the light curve is slightly smeared by this effect.

## 4. TEMPERATURE AND RADIUS

The color temperature of the companion can be calculated by using the magnitudes measured in the two bands. There were no detections in *I* near the *R* maximum because of the intermittent cloud. However, the lack of variation in the $V-R$ color of the companion to PSR B1957+20 within binary phase $\phi = \pm 0.3$ of companion conjunction (Callanan et al. 1995) suggests that the color measured at phase $\phi = 0.94$ for PSR J2051−0827, should be a good representation of the color at maximum. An *R* magnitude at $\phi = 0.94$ was calculated by interpolating between the detections at $\phi = 0.867$ and 0.975, giving $R - I = 0.69 \pm 0.17$. Using the cool M-type dwarf relations of Bessell (1995b) the effective temperature range corresponding to the $R - I$ color is $T_{\rm eff} = 4000$–$4700$ K.

The dispersion-measure–derived distance, $d = 1.3 \pm 0.4$ kpc, gives an absolute *R* magnitude of the companion at maximum of $M_R = 11.74^{+0.8}_{-0.6}$. Using Bessell's relations between $R - I$ and $M_{\rm bol}$ for M dwarfs (Bessell 1995b) the bolometric magnitude at maximum is $M_{\rm bol} = 11.75^{+0.8}_{-0.6}$ and the bolometric luminosity ranges from $0.76 \times 10^{-3}$ to $2.75 \times 10^{-3}$ $L_\odot$.

To estimate the radius of the companion that these luminosity and temperature ranges imply, we consider the area, *A*, illuminated by the impinging flux and use the standard relation $L = A\sigma T_{\rm eff}^4$. This area can be approximated by considering that the angle between the point on the surface of the star,

TABLE 1

MAGNITUDES OF COMPANION TO PSR J2051−0827

| Phase | Filter | Magnitude | Error |
|---|---|---|---|
| 0.544..... | *R* | 23.10 | 0.10 |
| 0.652..... | *R* | 22.62 | 0.08 |
| 0.760..... | *R* | 22.34 | 0.06 |
| 0.867..... | *R* | 22.71 | 0.07 |
| 0.975..... | *R* | 23.24 | 0.13 |
| 0.939..... | *I* | 22.37 | 0.14 |
| 0.047..... | *I* | 23.19 | 0.30 |

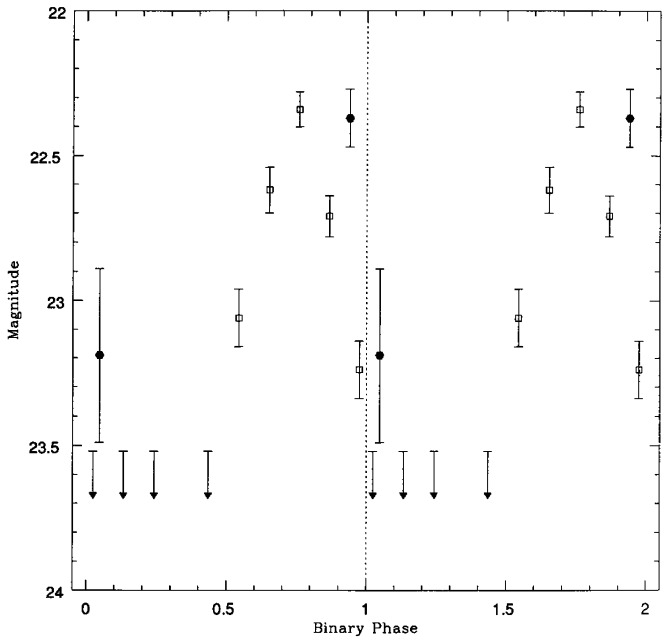


FIG. 2.—Phased light curve of the companion star to PSR J2051−0827 in both the $R$ (*squares*) and $I$ (*filled hexagons*) bands. The arrows indicate the upper limits on those $R$-band frames where the companion was not detected. The data points are repeated on the right-hand side of the dashed line to elucidate the shape of the light curve.

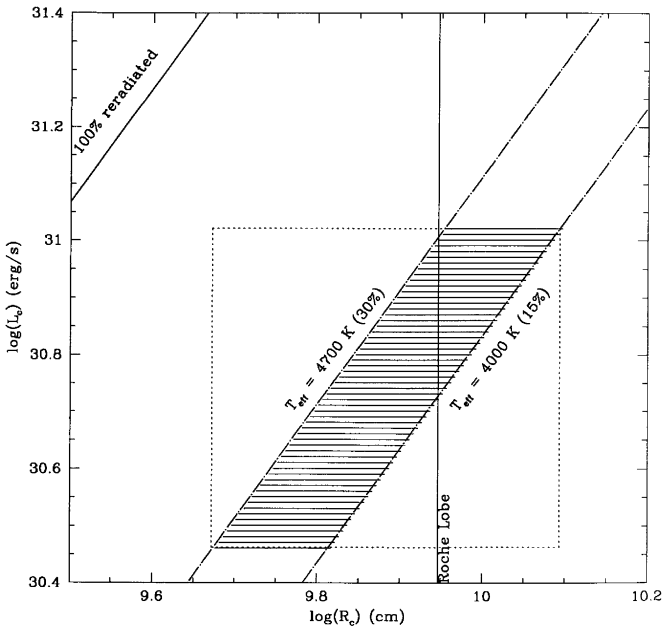


FIG. 3.—Percentage of impinging pulsar flux which must be reradiated to give the observed temperature. The dashed lines indicate the limiting values of companion radius $R_c$ and companion luminosity $L_c$, while the hatched region is the complete range of possible combinations of both that lie in the measured temperature range.

assumed spherical, at which the incident flux is zero and a line between the companion and pulsar centers is approximately 75°. Hence the illuminated, and optically reradiating, area can be approximated by a cap, $A = 1.5\pi r^2$. The corresponding range in radii is then 0.067–0.18 $R_\odot$ (the large range in radii is because of the combinations of extreme values of luminosity, temperature, and distance). Despite the large uncertainty in the radius, these observations indicate that the optical emitting region is likely to be of a similar size to the Roche lobe for the 0.027 $M_\odot$ companion (0.126 $R_\odot$). The theoretical radii of a degenerate H and He white dwarf are 0.1 and 0.043 $R_\odot$ (Shapiro & Teukolsky 1983), respectively, whereas we expect a nondegenerate star of the same mass to have a radius of approximately 0.1 $R_\odot$ (Burrows et al. 1993). Unfortunately the optical observations do not constrain the precise nature of the companion, but they do indicate that in order for the companion to fill its Roche lobe it will need to be bloated, either by interaction with the pulsar wind or by tidal forces.

## 5. DISCUSSION

As the size of the emitting region is the same as that which intersects the impinging pulsar flux we can place constraints on the ratio of $L_c/R_c^2$ to $L_{\rm inc}/R_c^2$, where $L_c$ is the companion luminosity, $L_{\rm inc}$ is the incident pulsar flux, and $R_c$ is the companion radius as shown in Figure 3. The bounding lines corresponding to the temperature limits indicate that this fraction lies in the range 15%–30%, which is somewhat larger than the 10%–20% of incident flux being reprocessed in the favored light-curve model of Callanan et al. (1995) for the PSR B1957+20 system. The shaded region of Figure 3 indicates the domain of all possible $L_c$ and $R_c$ values.

These calculations assume that the reprocessing of the impinging flux of the pulsar dominates the luminosity of the companion. If tidal forces (Applegate & Shaham 1994), such as those proposed to explain the variable orbital period derivative of PSR B1957+20, are active in the companion to PSR J2051−0827, then they would generate an internal luminosity. At present the back-side luminosity, believed to be representative of the internal luminosity, of the companion is rather poorly constrained, but the ratio of the Roche lobe radii of PSR B1957+20 and PSR J2051−0827 is ∼4. Therefore, the extreme power-law dependence of the tidal luminosity will enable comparisons to be made between the back-side temperatures of PSR B1957+20 and PSR J2051−0827 which will constrain models extremely effectively.

## REFERENCES

Applegate, J. H., & Shaham, J. 1994, ApJ, 436, 312
Arzoumanian, Z., Fruchter, A. S., & Taylor, J. H. 1994, ApJ, 426, L85
Banit, M., & Shaham, J. 1992, ApJ, 388, L19
Bessell, M. S. 1995a, PASP, 107, 672
———. 1995b, in Bottom of the Main Sequence and Beyond, ed. C. G. Tinney (Heidelberg: Springer), 123
Bhattacharya, D., & van den Heuvel, E. P. J. 1991, Phys. Rep., 203, 1
Burrows, A., Hubbard, W. B., Saumon, D., & Lunine, J. 1993, ApJ, 406, 158
Burstein, D., & Heiles, C. 1982, AJ, 87, 1165
Callanan, P. J., van Paradijs, J., & Rengelink, R. 1995, ApJ, 439, 928
Djorgovski, S., & Evans, C. R. 1988, ApJ, 335, L61
Fruchter, A. S., & Goss, W. M. 1992, ApJ, 384, L47
Fruchter, A. S., Gunn, J. E., Lauer, T. R., & Dressler, A. 1988a, Nature, 334, 686
Fruchter, A. S., Stinebring, D. R., & Taylor, J. H. 1988b, Nature, 333, 237
Landolt, A. U. 1992, AJ, 104, 372
Rasio, F. A., Shapiro, S. L., & Teukolsky, S. A. 1989, ApJ, 342, 934
Ryba, M. F., & Taylor, J. H. 1991, ApJ, 380, 557
Savage, B. D., & Mathis, J. S. 1979, ARA&A, 17, 73
Shapiro, S. L., & Teukolsky, S. A. 1983, Black Holes, White Dwarfs and Neutron Stars: The Physics of Compact Objects (New York: Wiley)
Stappers, B. W., et al. 1996, ApJ, 465, L119
Taylor, J. H., & Cordes, J. M. 1993, ApJ, 411, 674
van den Heuvel, E. P. J., & van Paradijs, J. 1988, Nature, 334, 227